

Synthesis and Site-Specific Incorporation of Red-Shifted Azobenzene Amino Acids into Proteins

Alford A. John, Carlo P. Ramil, Yulin Tian, Gang Cheng[†] and Qing Lin*

Department of Chemistry, State University of New York at Buffalo, Buffalo, New York 14260-3000, United States

Supporting Information

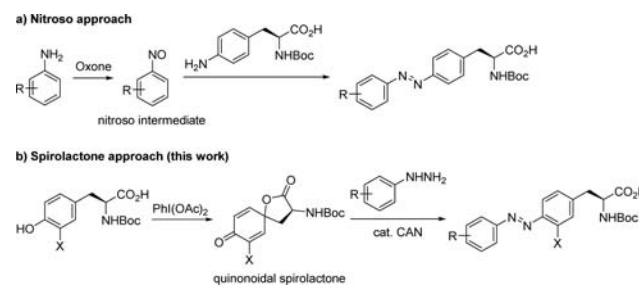
ABSTRACT: A series of red-shifted azobenzene amino acids were synthesized in moderate-to-excellent yields via a two-step procedure in which tyrosine derivatives were first oxidized to the corresponding quinonoidal spirolactones followed by ceric ammonium nitrate-catalyzed azo formation with the substituted phenylhydrazines. The resulting azobenzene–alanine derivatives exhibited efficient *trans/cis* photoswitching upon irradiation with a blue (448 nm) or green (530 nm) LED light. Moreover, nine superfolder green fluorescent protein (sfGFP) mutants carrying the azobenzene–alanine analogues were expressed in *E. coli* in good yields via amber codon suppression with an orthogonal tRNA/PylRS pair, and one of the mutants showed durable photoswitching with the LED light.



Until recently, the use of azobenzene photoswitches in biological systems typically required short-wavelength UV light in order to induce isomerization of the azo bond, which is undesirable because of the phototoxicity to cells. To minimize phototoxicity and reduce light scattering, recent efforts have focused on the design of highly substituted red-shifted azobenzenes.¹ On the basis of an earlier observation² that bulky substituents at the *ortho* positions of the azo bond caused a red shift in the $n \rightarrow \pi^*$ band and a blue shift in the $\pi \rightarrow \pi^*$ band, Woolley³ and Bléger⁴ designed tetra-*o*-methoxy- and tetra-*o*-fluoro-substituted, red-shifted azobenzenes, respectively, that showed robust photoswitching properties with the use of visible light. On the other hand, three strategies have been employed to introduce the azobenzenes into proteins site-selectively for the photoregulation of protein function in vivo. These include the design of the cysteine-reactive tethered ligands,^{5,6} the genetic encoding of the azobenzene amino acids in *E. coli*⁷ and mammalian cells,⁸ and the use of bioorthogonal ligation with genetically encoded bioorthogonal reporters.⁹ Among them, the genetic encoding of azobenzene amino acids is particularly attractive as it offers the highest incorporation efficiency in vivo without interference from intracellular thiols as well as potential side reactions found in bioorthogonal reactions. In addition, a genetically encoded azo bridge for proteins was reported recently, showing potentially improved photo control of protein function in vivo.¹⁰

To expand genetically encodable azobenzene photoswitches for photochemical control of protein function in vivo, efficient synthetic methods need to be developed. Previously, the azobenzene amino acids were prepared by treating anilines with Oxone to generate the nitrosobenzene intermediates, which reacted with the *p*-aminophenylalanine to afford the protected azobenzene amino acids in moderate yields (Scheme 1a).^{7,8} Since the nitroso intermediates are unstable and the *p*-aminophenylalanine analogues are not widely available, alternative synthetic methods are highly desirable. Herein, we

Scheme 1. Approaches for Synthesis of Azobenzene Amino Acids

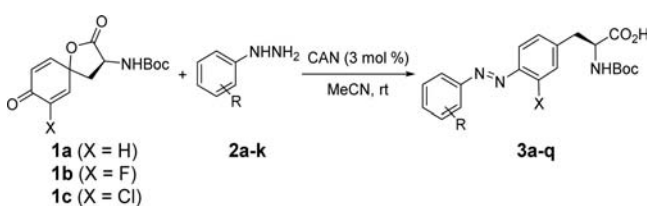


report the facile synthesis of the highly substituted azobenzene amino acids through the reaction of quinonoidal spirolactones, which can be prepared in one step from the tyrosines, and phenylhydrazines in the presence of ceric ammonium nitrate (CAN) catalyst (Scheme 1b). Furthermore, nine new azobenzene amino acids were incorporated into the superfolder green fluorescent protein (sfGFP) in *E. coli* using a reported orthogonal tRNA/PylRS pair. One of the resulting azo-sfGFP showed durable photoswitching with the LED light.

In search of efficient methods for the synthesis of azobenzene amino acids, we were intrigued by a report from Carreño and co-workers where they showed that the azobenzenes can be prepared in good-to-excellent yields from quinone bisacetals and arylhydrazines in the presence of a catalytic amount of CAN.¹¹ To examine whether this method can be extended to the quinone analogue derived from tyrosine, we prepared the quinonoidal spirolactone 1a (structure in Table 1 scheme) in 37% yield by treating *N*-Boc-*L*-tyrosine with a slight excess amount of phenyliodonium diacetate (PIDA).¹² Separately, the

Received: November 12, 2015

Published: December 9, 2015

Table 1. Synthesis of *N*-Boc-Protected Azobenzene–Alanine Analogues

entry	X	R	product	yield ^a (%)
1	H	4-Me (2a)	3a	73
2	H	2-OMe (2b)	3b	72
3	H	4-CN (2c)	3c	72
4	H	3-CN (2d)	3d	85
5	H	3-CH=CH ₂ (2e)	3e	68
6	H	3-C≡CH (2f)	3f	83 ^b
7	H	2,6-F ₂ (2g)	3g	95
8	H	2,4,6-F ₃ (2h)	3h	91
9	H	2,6-F ₂ -4-CONH ₂ (2i)	3i	94 ^c
10	H	2,6-F ₂ -4-I (2j)	3j	82 ^{d,e}
11	H	2,3,4,5,6-F ₅ (2k)	3k	89
12	F	2,6-F ₂ (2g)	3l	72
13	F	2,4,6-F ₃ (2h)	3m	72
14	F	2,3,4,5,6-F ₅ (2k)	3n	60
15	Cl	2,6-F ₂ (2g)	3o	68 ^{e,f}
16	Cl	2,4,6-F ₃ (2h)	3p	67 ^{f,g}
17	Cl	2,3,4,5,6-F ₅ (2k)	3q	63

^aIsolated yields were reported. Unless noted otherwise, reactions were carried out by stirring a solution of spirolactone (**1a–c**) with 1.1 equiv of the substituted phenylhydrazine in MeCN at room temperature for 12–17 h. ^b24 h reaction time. ^cMeOH/MeCN (1:4) was used as solvent. ^d1.5 equiv of the substituted phenylhydrazine was used. ^e72 h reaction time. ^f2.5 equiv of the substituted phenylhydrazine was used. ^g48 h reaction time.

phenylhydrazine derivatives are either commercially available or can be readily prepared from appropriate anilines through the diazonium salt formation followed by reduction with SnCl₂ in HCl.¹³

With the substrates in hand, we performed the azo formation reaction in acetonitrile in the presence of 3 mol % of CAN, and the results are summarized in **Table 1**. For monosubstituted phenylhydrazines **2a–f**, the *N*-Boc-protected *trans*-dominant azobenzene–alanines were obtained in 68–85% yield (entries 1–6, **Table 1**) with no obvious electronic and steric effects. The vinyl group at the *meta* position in the azo product **3e** might

provide a potential cross-linking site for a proximal cysteine (e.g., at the *i*+7 position) through the thiol–ene click reaction as reported.¹⁴ Similarly, the acetylene moiety at the *meta* position of **3f** offers a bioorthogonal handle for conjugation with an azide-containing ligand via either copper-catalyzed click chemistry¹⁵ or copper-catalyzed Glaser–Hays bioconjugation reaction.¹⁶ Since Bléger et al. showed that *o*-fluorine substitution leads to superior photoswitching properties,⁴ we investigated the reactivity of a series of fluorine-substituted phenylhydrazines **2g–k** in the CAN-catalyzed azo formation reaction. To our satisfaction, the fluorinated azobenzene–alanine analogues were obtained in good to excellent yields (entries 7–11, **Table 1**), irrespective of the number of fluorines as well as additional substituents.

Since the *ortho*-substituted azobenzenes show red-shifted absorbance and improved photophysical properties compared to the azobenzene parent, we chose two commercially available *ortho*-halogenated *L*-tyrosine derivatives and prepared their corresponding quinonoidal spirolactones, **1b** and **1c**, using the PIDA method (structures are shown in the **Table 1** scheme). To maximize potential improvement in photophysical properties, these two spirolactones were reacted with the *ortho*-difluorinated phenylhydrazines **2g**, **2h**, and **2k**. All six halogenated azobenzene–alanine products **3l–q** were obtained uneventfully in moderate yields (entries 12–17, **Table 1**), though longer incubation times were required for the two chlorinated azo products, presumably due to the bulky chlorine substituent that slows down the nucleophilic addition.

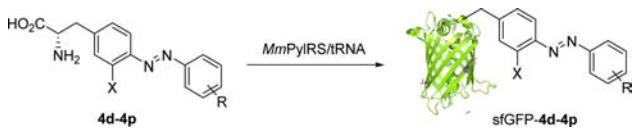
Because the *ortho*-fluorinated azobenzenes were reported to show good separation of *trans/cis* $n \rightarrow \pi^*$ bands, and as a result achieve high *cis* and *trans* photostationary state (pss),⁴ we investigated photoswitching properties of nine fluorinated azobenzene–alanine analogues we synthesized. The simplest difluorinated azobenzene analogue, **3g**, showed a wavelength separation of 8 nm and 66% *cis* and 62% *trans* pss after 30 min photoirradiation with green (530 nm) and blue (448 nm) LED light, respectively (**Table 2**). Adding additional fluorine on one side of the azo bond increased the wavelength separation but led to lower *cis*-pss (compare **3h** and **3k** to **3g** in **Table 2**). When a fluorine was introduced in the *ortho* position of the internal benzene ring, all three tri-*ortho*-fluorinated azobenzene–alanine analogues (**3l**, **3m**, and **3n**) showed greater wavelength separation (12–16 nm) than **3g**; most strikingly, **3m** exhibited 76% *cis*-pss after irradiation with green light. However, when a chlorine was placed at the *ortho* position of the internal benzene ring, divergent behaviors were observed

Table 2. Photophysical Properties of *N*-Boc-Protected Azobenzene–Alanine Analogues

compd	X	R	<i>trans</i> $\lambda_{\max} n \rightarrow \pi^*$ (nm)	<i>cis</i> $\lambda_{\max} n \rightarrow \pi^*$ (nm)	$n \rightarrow \pi^*$ separation ^a (nm)	<i>trans:cis</i> 530 nm	<i>trans:cis</i> 448 nm
3g	H	2,6-F ₂	435	427	8	34:66 ^b	62:38 ^b
3h	H	2,4,6-F ₃	439	429	10	38:62 ^c	61:39 ^c
3k	H	2,3,4,5,6-F ₅	446	428	18	43:57 ^c	64:36 ^c
3l	F	2,6-F ₂	442	426	16	36:64 ^b	60:40 ^b
3m	F	2,4,6-F ₃	436	424	12	24:76 ^b	61:39 ^b
3n	F	2,3,4,5,6-F ₅	442	429	13	35:65 ^c	62:38 ^c
3o	Cl	2,6-F ₂	428	426	2	23:77 ^b	70:30 ^b
3p	Cl	2,4,6-F ₃	425	425	0	28:72 ^b	71:29 ^b
3q	Cl	2,3,4,5,6-F ₅	448	434	15	34:66 ^b	67:33 ^b

^aWavelength separation was calculated using the following equation: $\Delta = \lambda_{\max,trans} - \lambda_{\max,cis}$. ^b*Trans/cis* ratio was determined by ¹⁹F NMR. ^c*Trans/cis* ratio was determined by ¹H NMR. Sample was dissolved in DMSO-*d*₆ in an NMR tube to obtain a concentration of 15–22 mM. The photoirradiation was performed by placing the NMR tube on top of an LED light in an enclosed compartment for 30 min.

Table 3. Genetic Incorporation of Azobenzene–Alanine Analogues into Superfolder GFP



compd	X	R	calcd mass, Da	obsd mass, Da	yield (mg/L)	% Gln incorp ^a
4d	H	3-CN	27856.3	27857.6 ± 1.3	32.0	0
4g	H	2,6-F ₂	27868.1	27867.6 ± 1.0	22.3	0
4h	H	2,4,6-F ₃	27886.1	27885.2 ± 0.9	31.6	0
4k	H	2,3,4,5,6-F ₅	27921.3	27920.3 ± 1.8	5.4	36
4l	F	2,6-F ₂	27886.1	27886.0 ± 1.1	10.2	4
4m	F	2,4,6-F ₃	27903.3	27901.9 ± 1.6	3.9	21
4n	F	2,3,4,5,6-F ₅	27941.1	27940.3 ± 1.7	4.8	50
4o	Cl	2,6-F ₂	27902.1	27904.6 ± 1.6	7.8	68
4p	Cl	2,4,6-F ₃	27920.5	27920.3 ± 1.2	4.4	27

^aThe Gln incorporation into sfGFP in the purified protein samples was calculated on the basis of ion counts using the following equation: $\text{Gln \%} = I_{\text{sfGFP-S2Q}} / (I_{\text{sfGFP-S2Q}} + I_{\text{sfGFP-S2} \rightarrow \text{Aba}})$, where $I_{\text{sfGFP-S2Q}}$ and $I_{\text{sfGFP-S2} \rightarrow \text{Aba}}$ are the ion counts of sfGFP-S2Q and sfGFP-S2 → Aba, respectively, in the deconvoluted mass spectra.

for the resulting three azobenzene–alanine analogs (**3o**, **3p**, and **3q**). For di- and trifluorinated analogues (**3o** and **3p**), there was hardly any separation for the $n \rightarrow \pi^*$ bands, but **3o** showed the highest *cis*-pss (77%) detected in the series along with the second highest *trans*-pss (70%). For **3q**, despite the largest bathochromic shift in the *trans* $n \rightarrow \pi^*$ band (448 nm) and improved wavelength separation compared to **3g**, the *cis*-pss remained unchanged while the *trans*-pss showed a modest improvement. It is noteworthy that the photostationary states were reached after only 5 min photoirradiation in a time–course study with **3h** (Table S1, Supporting Information) and that the *cis*-pss of **3h** did not show measurable reduction after 4 days of dark adaptation at room temperature (Figure S1, Supporting Information). Taken together, there was no apparent correlation between the wavelength separation and the pss, suggesting an alternative mechanism may be needed to account for this discrepancy. Unexpectedly, the *o*-chlorine-substituted di-*o*-fluoroazobenzene–alanine analogues **3o** and **3p** exhibited essentially no wavelength separation but highest *cis*- and *trans*-pss values, the parameters most relevant in photochemical control of protein function in biological system.

Since several substituted azobenzene–alanines have been site-specifically incorporated into proteins using amber codon suppression with the orthogonal *MmPylRS*/tRNA_{CUA} pairs,⁸ we surmised that our new azobenzene–alanine analogues could be similarly incorporated into proteins using the same system. Accordingly, *pEvol-PylT-MmPylRS* plasmid encoding a Pyl-tRNA_{CUA} and a PylRS variant carrying four mutations (A302T, L309S, N346V, and C348G) in its active site was prepared and then cotransformed into BL21(DE3) cells along with the pET-sfGFP-S2TAG reporter plasmid. The resulting transformants were grown in 10 mL LB medium supplemented with 1 mM azobenzene–alanine (Aba) analogue at 37 °C, and the Aba-encoded sfGFP proteins were isolated through Ni–NTA affinity chromatography. Among the azobenzene–alanine analogues tested, small substituents on the distal benzene ring such as cyano and fluorine are generally well accepted by the synthetase with expression yields reaching as high as 32.0 mg L⁻¹ (Table 3), along with high fidelity evidenced by mass spectrometry (see the Supporting Information). One exception is pentafluoro analogue **4k**, which produced a lower yield of 5.4 mg L⁻¹ with 36% near-cognate Gln-suppression product,¹⁷ indicating the *m*-fluoro substituents are not well tolerated by

the synthetase. When the *o*-fluorine was introduced into the internal benzene ring, the azobenzene–alanine derivatives (**4l**, **4m**, and **4n**) showed lower expression yields, along with the erosion of fidelity. A similar phenomenon was also observed for the *ortho*-substituted azobenzene–alanine analogues **4o** and **4p**, presumably due to the repulsion between the internal halogen and the distal azo-nitrogen, which twists the azo bond out of coplanarity with the internal benzene ring⁴ resulting in poorer substrate properties. With these observations, it appears that new PylRS variants are warranted in order to efficiently charge the twisted tri-*o*-halogenated azobenzene–alanines with high fidelity in *E. coli*.

To examine whether the genetically encoded azobenzenes in proteins can respond to visible-light induced photoswitching, we subjected the highly expressed sfGFP mutant sfGFP–**4h** to alternating 5 min green-blue irradiation cycles and monitored the $\pi \rightarrow \pi^*$ bands (Figure S2, Supporting Information) because of their relatively high intensity in the UV–vis spectra. Closer examination revealed rhythmic changes in absorbance at 340 nm over 10 cycles, consistent with reversible photoswitching between the *trans* (high absorbance at 340 nm) and *cis* (low absorbance at 340 nm) form of the azo bond with no sign of “fatigue”, the erosion of *cis* ratio during photoswitching cycles (Figure 1). The photoswitching durability of the trifluorinated azobenzene in sfGFP–**4h** also highlighted an exceptional photostability for the fluorinated azobenzene system.⁴

In summary, we have synthesized a series of red-shifted azobenzene–alanine analogues from the substituted tyrosine and phenylhydrazine derivatives via a two-step procedure. The route involves storable spirolactone intermediates and enables facile unsymmetrical azo formation with the phenylhydrazines in the presence of the ceric ammonium nitrate catalyst. The photophysical properties of the fluorinated azobenzene–alanine analogues were characterized, with the *o*-chlorodifluoroazobenzene **3o** reaching the highest photostationary states (77% *cis*-pss after 530 nm photoirradiation and 70% *trans*-pss after 448 nm photoirradiation). In addition, nine azobenzene–alanine amino acids were genetically incorporated into proteins in *E. coli* with good-to-excellent yields and varying degrees of fidelity via amber codon suppression with an orthogonal tRNA/PylRS pair; eight of them are reported here for the first time. One azobenzene-containing protein, sfGFP–**4h**, showed durable photoswitching upon photoirradiation with alternating green–

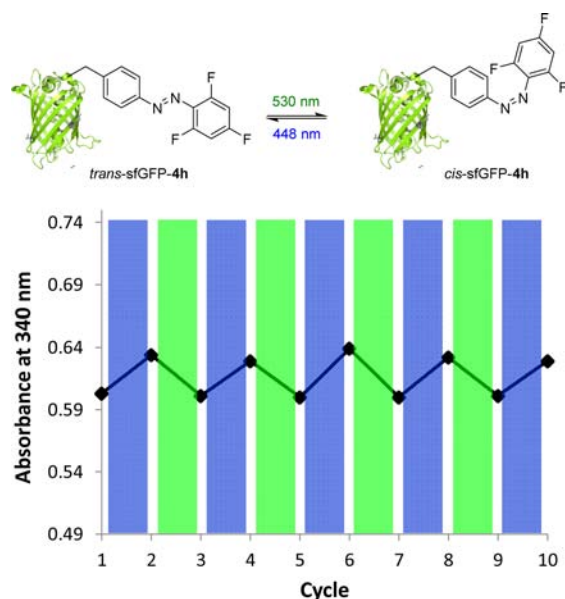


Figure 1. Reversible photoswitching of sfGFP-4h in PBS buffer with alternating 530/448 nm LED photoirradiation.

blue LED light. The successful development of the spiroactone approach to azobenzene amino acid synthesis, in conjunction with continuous evolution of additional azobenzene–alanine-specific tRNA/PyIRS pairs, should greatly enhance our capability to harness the power of azobenzene photoswitches for the photochemical regulation of protein function in vivo with a high spatiotemporal precision.

■ ASSOCIATED CONTENT

Supporting Information

The Supporting Information is available free of charge on the ACS Publications website at DOI: 10.1021/acs.orglett.5b03268.

Supplemental figures, experimental procedure, and characterization of all new compounds (PDF)

■ AUTHOR INFORMATION

Corresponding Author

*E-mail: qinglin@buffalo.edu.

Present Address

†Zhejiang University, College of Pharmaceutical Sciences, China.

Notes

The authors declare no competing financial interest.

■ ACKNOWLEDGMENTS

We gratefully acknowledge the National Institutes of Health (GM 85092) for financial support. We thank Prof. Wenshe Liu at Texas A&M University for providing the pEvol-MmPyIRS and pET-sfGFPS2TAG plasmids and Tracey Lewandowski in the Q.L. lab at SUNY Buffalo for assistance with cloning.

■ REFERENCES

- (1) Dong, M.; Babalhavaeji, A.; Samanta, S.; Beharry, A. A.; Woolley, G. A. *Acc. Chem. Res.* **2015**, *48*, 2662–2670.
- (2) Forber, C. L.; Kelusky, E. C.; Bunce, N. J.; Zerner, M. C. *J. Am. Chem. Soc.* **1985**, *107*, 5884–5890.

- (3) Beharry, A. A.; Sadovski, O.; Woolley, G. A. *J. Am. Chem. Soc.* **2011**, *133*, 19684–19687.

- (4) Bléger, D.; Schwarz, J.; Brouwer, A. M.; Hecht, S. *J. Am. Chem. Soc.* **2012**, *134*, 20597–20600.

- (5) Bartels, E.; Wassermann, N. H.; Erlanger, B. F. *Proc. Natl. Acad. Sci. U. S. A.* **1971**, *68*, 1820–1823.

- (6) Banghart, M.; Borges, K.; Isacoff, E.; Trauner, D.; Kramer, R. H. *Nat. Neurosci.* **2004**, *7*, 1381–1386.

- (7) Bose, M.; Groff, D.; Xie, J.; Brustad, E.; Schultz, P. G. *J. Am. Chem. Soc.* **2006**, *128*, 388–389.

- (8) Hoppmann, C.; Lacey, V. K.; Louie, G. V.; Wei, J.; Noel, J. P.; Wang, L. *Angew. Chem., Int. Ed.* **2014**, *53*, 3932–3936.

- (9) Tsai, Y.-H.; Essig, S.; James, J. R.; Lang, K.; Chin, J. W. *Nat. Chem.* **2015**, *7*, 554–561.

- (10) Hoppmann, C.; Maslennikov, I.; Choe, S.; Wang, L. *J. Am. Chem. Soc.* **2015**, *137*, 11218–11221.

- (11) Carreño, M. C.; Mudarra, G. F.; Merino, E.; Ribagorda, M. J. *Org. Chem.* **2004**, *69*, 3413–3416.

- (12) Rama Rao, A. V.; Gurjar, M. K.; Sharma, P. A. *Tetrahedron Lett.* **1991**, *32*, 6613–6616.

- (13) Hunsberger, I. M.; Shaw, E. R.; Fugger, J.; Ketcham, R.; Lednicer, D. *J. Org. Chem.* **1956**, *21*, 394–399.

- (14) Hoppmann, C.; Kühne, R.; Beyermann, M. *Beilstein J. Org. Chem.* **2012**, *8*, 884–889.

- (15) Chandrasekaran, V.; Lindhorst, T. K. *Chem. Commun.* **2012**, *48*, 7519–7521.

- (16) Lampkowski, J. S.; Villa, J. K.; Young, T. S.; Young, D. D. *Angew. Chem., Int. Ed.* **2015**, *54*, 9343–9346.

- (17) Odoi, K. A.; Huang, Y.; Rezenom, Y. H.; Liu, W. R. *PLoS One* **2013**, *8*, e57035.